Clim. Past, 10, 1109–1123, 2014
www.clim-past.net/10/1109/2014/
doi:10.5194/cp-10-1109-2014

Climate of the Past
Open Access

Past freeze and thaw cycling in the margin of the El'gygytgyn crater deduced from a 141 m long permafrost record

G. Schwamborn[1], **H. Meyer**[1], **L. Schirrmeister**[1], **and G. Fedorov**[2,3]

[1]Alfred Wegener Institute, Helmholtz Centre for Polar and Marine Research, Telegrafenberg A43, 14473 Potsdam, Germany
[2]Arctic and Antarctic Research Institute, Bering Street 38, 199397 St. Petersburg, Russia
[3]St. Petersburg State University, 10 line V.O., 33, 199178 St. Petersburg, Russia

Correspondence to: G. Schwamborn (georg.schwamborn@awi.de)

Received: 14 June 2013 – Published in Clim. Past Discuss.: 16 July 2013
Revised: 3 March 2014 – Accepted: 16 April 2014 – Published: 10 June 2014

Abstract. The continuous sediment record from Lake El'gygytgyn in the northeastern Eurasian Arctic spans the last 3.6 Ma and for much of this time permafrost dynamics and lake level changes have likely played a crucial role for sediment delivery to the lake. Changes in the ground-ice hydrochemical composition ($\delta^{18}O$, δD, pH, electrical conductivity, Na^+, Mg^{2+}, Ca^{2+}, K^+, HCO_3^-, Cl^-, SO_4^-) of a 141 m long permafrost record from the western crater plain are examined to reconstruct repeated periods of freeze and thaw at the lake edge. Stable water isotope and major ion records of ground ice in the permafrost reflect both a synsedimentary palaeo-precipitation signal preserved in the near-surface permafrost (0.0–9.1 m core depth) and a post-depositional record of thawing and refreezing in deeper layers of the core (9.1–141.0 m core depth). These lake marginal permafrost dynamics were controlled by lake level changes that episodically flooded the surfaces and induced thaw in the underlying frozen ground. During times of lake level fall these layers froze over again. At least three cycles of freeze and thaw are identified and the hydrochemical data point to a vertical and horizontal talik refreezing through time. Past permafrost thaw and freeze may have destabilised the basin slopes of Lake El'gygytgyn and this has probably promoted the release of mass movements from the lake edge to the deeper basin as known from frequently occurring turbidite layers in the lake sediment column.

1 Introduction

The water level of Lake El'gygytgyn, which developed in the 3.6 million year old impact crater in the Eurasian Arctic (Layer, 2000), has changed several times, at least during the late Quaternary as indicated by subaerial and subaquatic lake terrace remnants (Glushkova and Smirnov, 2007; Schwamborn et al., 2008; Juschus et al., 2011). Recently the basin fill was cored and a unique 312 m long Pliocene–Pleistocene lake sediment record (core 5011-1) was retrieved, which is being explored for palaeoclimatic and palaeoenvironmental reconstruction (Melles et al., 2012; Brigham-Grette et al., 2013). Additionally, a 141 m long permafrost core (core 5011-3) was taken from the western crater margin for studying catchment–lake interaction in the past (Fig. 1). Interpretation of the permafrost core sediments suggests that there is a close linkage between alluvial fan growth on the slopes and the sediment delivery to the lake; in modern times the seasonal (i.e. snow-melt related) sediment transport removes sediment basinward from the subaerial plain into the subaqueous fan and basin floor environments and this is also interpreted for much of the geologic past in this Arctic setting even though core 5011-3 is poorly dated (Schwamborn et al., 2012a). Age control exists only for the upper 9.6 m of core where an Allerød (AD)–Younger Dryas (YD)–Holocene sequence is preserved based on the pollen record (Andreev et al., 2012). The more ancient part of the core includes non-dated slope and alluvial deposits with unknown sedimentation rates and dis- and unconformities (Fig. 2). The prograding sediment transport in alluvial fan systems on the western lake edge has probably initiated frequent sliding events into the lake basin as found in seismic lines (Niessen et al., 2007) and in lake cores (Juschus et al., 2009). Recently, 37 % of the Quaternary sediment series in lake core 5011-1 were found to consist of mass movement deposits (Sauerbrey et al., 2013). Next to prograding sediment transport permafrost

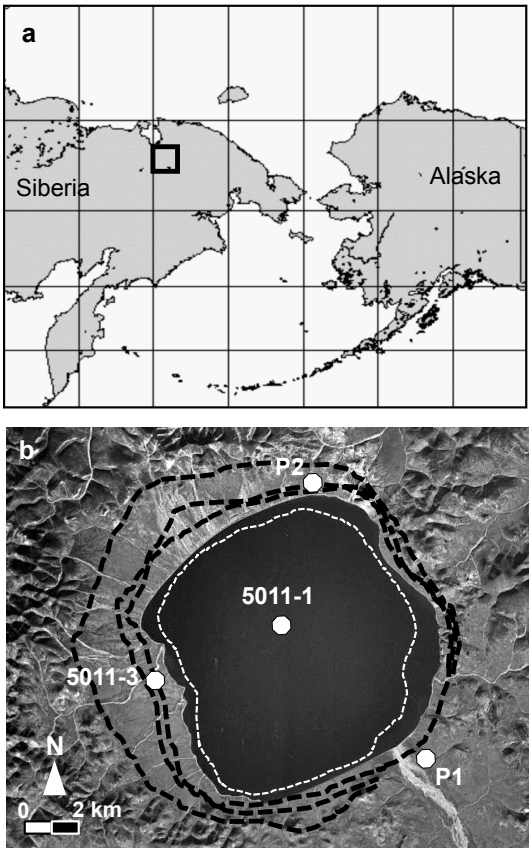

Figure 1. (a) Geographic position of the El'gygytgyn crater in NE Russia (black box). **(b)** A Corona image (source: USGS) showing Lake El'gygytgyn and drill sites 5011-3 on the permafrost flat west of the lake and 5011-1 in the lake. Dashed black lines indicate shorelines of the Middle Pleistocene (outer) and the Late Pleistocene (middle) according to Glushkova and Smirnov (2007), and the Allerød (inner) based on Schwamborn et al. (2008). The inner broken white line indicates the shoreline of the LGM according to Juschus et al. (2011). P1 and P2 denote the location of the short permafrost cores discussed in the text.

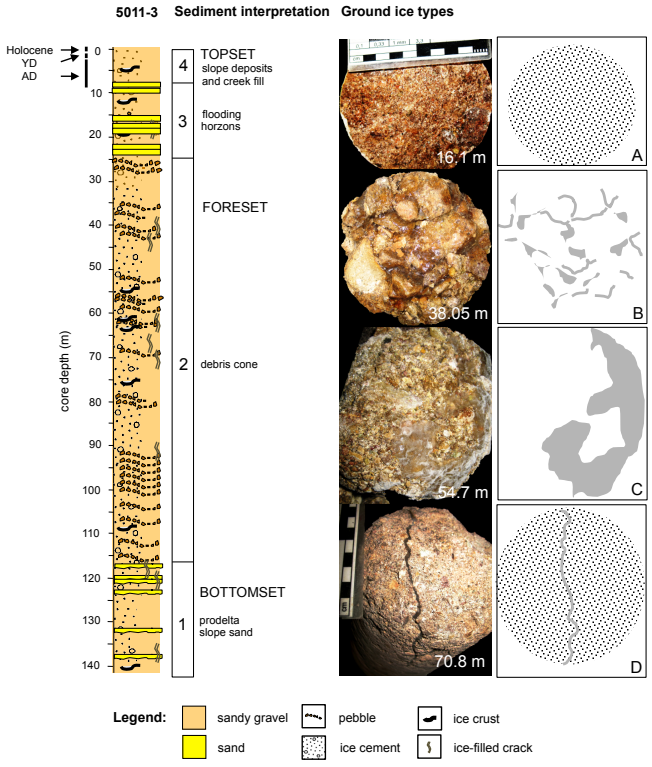

Figure 2. Left: the lithological log of core 5011-3 including pollen-based stratigraphy from Andreev et al. (2012) and sediment interpretation from Schwamborn et al. (2012a); YD = Younger Dryas, AD = Allerød. Right: photographic examples and generalised cryotexture of ground ice in the core. The scale is in cm, the core diameter is 11 cm. **(A)** ice cement in a sandy matrix, **(B)** pore space fillings in a pebble layer, **(C)** ice crust around sandy gravel, **(D)** near-vertical ice vein in sandy gravel.

thaw and freeze might be another cause of sediment release to the basin, because during periods of rising lake level the marginal permafrost thaws in the inundated areas and material might become destabilised where slopes are steep. In order to better understand the permafrost-dependent (i.e. freezing-front dependent) sediment delivery to the basin, determining the ground-ice composition and its origin helps to complete the understanding of the lake marginal depositional history. Today's catchment-to-lake ratio is only 1.6 : 1, but the catchment size has changed during the Quaternary based on geomorphic studies of terraces in the area (e.g. Glushkova and Smirnov, 2007) and lake level changes potentially exerted a large influence on the amount and nature of material released into the basin.

The history of talik development (i.e. an unfrozen zone below the lake surrounded by permafrost) is likely stored in the permafrost pore water chemistry; the study of this chemistry in order to elucidate the history is the subject of this paper. The stable isotope composition in the ground ice of core 5011-3 can give evidence on water origin (precipitation versus lake water) and isotope modification through fractionation during phase transitions (i.e. freezing). Under peculiar conditions the ground ice also may have preserved a climatic signal (see Schwamborn et al., 2006). Variations of the stable water isotope composition in natural environments have been widely used in the interpretation of past polar climatic and environmental conditions. Ground ice has been analysed to infer climate history in non-glaciated terrain (Meyer et al., 2010a, b; Opel et al., 2011) or to elucidate the origin of Antarctic permafrost (Stuiver and Yang, 1981; Swanger et al., 2010). Other ground-ice research has been used to infer combined palaeoenvironmental and palaeoclimatic change in the terrestrial Arctic (Mayer et al., 2002a, b; Lacelle et al., 2004; Wetterich et al., 2011; Vasil'chuk et al., 2012) or to aid the genetic interpretation of water sources in permafrost terrain (e.g. Mackay, 1983; Leibman, 1996; Dereviagin et al., 2003; Lacelle et al., 2004, 2009).

Permafrost aggradation at any given site is accompanied by pore water freezing in situ or migrating to form ice lenses. Ion and O–H isotope fractionation are known to be affected by freezing and diffusion rates (Souchez et al., 2000; Lacelle et al., 2009; Fritz et al., 2011; Michel, 2011); therefore, the first ice to form will have heavier δ^{18}O and δD values (and a lower d excess) than the last ice. Gradients are expected to result from lateral, down or upward permafrost growth even in homogenous material with an initial uniform groundwater quality. Following Lacelle (2011), the first ice to form will be enriched in ^{18}O by about 3 ‰ (and about 20 ‰ in D) as freezing begins, but as freezing continues, the δ^{18}O composition of the forming ice becomes progressively depleted as the δ^{18}O composition of the residual water trends toward lower values. Conversely, freezing of liquid water leads to a progressive increase in d excess even to values of > 10 ‰ above the global meteoric water line (GMWL) (Fritz et al., 2011).

There have been various attempts to correlate and explain the co-isotope slopes of ice and water frozen under a variety of conditions. As noted in Mackay (1998, and references cited therein), the slopes alone have usually been difficult to interpret in both glacial and periglacial studies. In all cases, it was recommended that stable O–H isotope measurements should be supported by the use of additional distinguishing tools as are discussed below when attempting to infer ground-ice genesis (Mayer et al., 2002b; Lacelle, 2011).

Changes in the downcore record of light soluble salts are one additional indicator of permafrost degradation and aggradation. When permafrost aggrades in moist sediments, the chemical composition of the newly formed ground ice differs from the unfrozen pore water. Previous studies show that ice formation is linked to solute redistribution, because solutes are excluded from the crystal lattice as water freezes (e.g. Mackay and Lavkulich, 1974; Hallet, 1978; Mahar et al., 1983; Kadlec, 1984; Ostroumov et al., 2001). This causes differentiated solute redistribution at permafrost sites with multiple but non-equal freeze and thaw cycles of different waters. A spatially inhomogeneous concentration pattern may thus reflect a differentiated retreat and advance of the freezing front, which causes a solute redistribution in the subground and variations in the ground-ice record. A prominent example is the active layer (i.e. seasonally thawed soil layer), where soil moisture is annually redistributed and the last soil layer to refreeze has the lowest δ values and the highest ion concentration (Ostroumov et al., 1998). Ground ice with low-soil solute concentration points to surfaces that were subject to progressive removal of soluble material as deeper permafrost thawed (Kokelj and Burn, 2005). Especially in freezing sandy environments the solutes migrate to the unfrozen zone (Qiu et al., 1988). However, if freezing takes place rapidly enough the leaching of saline pore water can be prevented almost completely as has been observed in emerged marine sediments (O'Sullivan, 1963).

The aim of this paper is to highlight a subject that has been little studied to date, the effect of sediment freezing on the pore water hydrochemical composition and the interpretation of connected past environmental change. This will help to advance our understanding of the long-term lake, alluvial (i.e. stream migration) and permafrost processes that have shaped the unique Lake El'gygytgyn archive. This paper complements the sedimentological approach of Schwamborn et al. (2012a) by focusing on the hydrochemical aspects (i.e. changes in stable water isotopes and in ion concentration) of the 5011-3 permafrost record.

2 Environmental setting

El'gygytgyn crater is a roughly circular depression, 18 km in diameter, and partially occupied by a lake that is 12 km in diameter (Fig. 1). The hills on the crater rim rise to between 600 and 930 m above sea level (a.s.l.), and the lake level is 492 m a.s.l. Fifty seasonally active inlet streams drain the crater slopes and loose Quaternary deposits cover the crater plain surrounding the lake. The active layer is about 0.4 m deep in peaty silts and can reach 0.5–0.8 m in sand and gravels on the slopes. The site is in the continuous permafrost zone with a MAAT (mean annual air temperature) of -10 °C at 3 m above the ground (Nolan and Brigham-Grette, 2007). Air temperature extremes in 2002 ranged from -40 to $+26$ °C and precipitation comprised 70 mm of summer rainfall (June–September) and 110 mm water equivalent of snow (Nolan and Brigham-Grette, 2007). The MAGT (mean annual ground temperature) below the area of seasonal temperature cycling is -6.1 °C at 20 m depth with a total permafrost thickness between 330 and 360 m calculated from borehole temperature measurements at site 5011-3 (Mottaghy et al., 2013).

Both beneath the surface and above the shoreline of the presently 170 m deep (at maximum) bowl-shaped lake there is a series of terrace remnants, which mark ancient shoreline positions. Glushkova and Smirnov (2007) mapped two ancient shorelines based on subaerial terrace remnants, which are tentatively attributed to the "Middle Pleistocene" at 35–40 m above the present lake level ($+40$ m terrace) and the "Late Pleistocene" at 9–11 m above the present lake level ($+10$ m terrace). Schwamborn et al. (2008) dated an Allerød (AD) lake level at 3–4 m above the present lake level ($+4$ m terrace). In addition, Juschus et al. (2011) recognised a subaquatic terrace at 10–12 m below the present lake level and attributed it to the "last glacial maximum (LGM)" (-10 m terrace).

The 5011-3 coring position (76°29.10′ N, 171°56.70′ E) is located in the central part of the western permafrost flat (Fig. 1). The core position lies 8 m higher than the lake level on a gently sloping surface ($< 4°$). To the east the closest shore bars are 350 m away, and to the west the nearest volcanic bedrock occurs 4 km upslope. The area between is covered by talus and slope material. A hummocky tundra environment characterises the surface with a loamy

to rubbly substrate. Surface drainage occurs mainly during spring snowmelt. The ground is mostly dry in summer. Creeks are intermittent and ponds do not persist. The coring site is located at the distal end of a sediment fan that is the most distinctive sediment body on the western-to-northern braid plain; several fans in a row cover this area (Schwamborn et al., 2012a).

3 Methods

Core 5011-3 reached a depth of 141 m with 91 % core recovery. The strata were entirely frozen when recovered. On site, the core sections were initially described and photographically documented. They were kept frozen in the field and during transport to the laboratory (where the cores were cleaned), the documentation was completed, and subsamples were taken from the sediment and the ground ice for further laboratory analyses. On average, samples were taken every 0.5 m or where a sediment change occurred. Sections were 15–20 cm long and had a gross weight of about 2–3 kg. Frozen samples stored in polyethylene bags were weighed, thawed, and allowed to settle. Thawed ground ice was immediately extracted from the samples using pore water samplers (i.e. rhizomes; Seeberg-Elverfeldt et al., 2005). The extracted water was analysed for pH and electrical conductivity (EC) using a WTW Multilab 540. Subsamples were taken for stable water isotope and main cation and anion analyses.

Hydrogen and oxygen isotope ratios were measured on a Finnigan MAT Delta-S mass spectrometer and are presented using δ notation representing the per mille (‰) relative difference with respect to Vienna standard mean ocean water (VSMOW). The measuring procedure is described in Meyer et al. (2000). Internal 1σ error is better than 0.1 % for δ^{18}O and 0.8 % for δD. The results are presented in δ^{18}O–δD diagrams with respect to the GMWL, a correlation of surface waters and precipitation with a slope of about 8 (GMWL; $\delta\mathrm{D} = 8\delta^{18}\mathrm{O} + 10$; Craig, 1961; Rozanski et al., 1993). In addition, the deuterium excess d ($d = \delta\mathrm{D} - 8\delta^{18}\mathrm{O}$; Dansgaard, 1964) gives evidence on the deviation from the GMWL and helps to elucidate the kinetic (i.e. non-equilibrium) fractionation processes. The d excess is affected by relative humidity during the formation of primary vapour masses. On a global scale, d excess for precipitation averages +10 ‰; it is reduced to values near 0 ‰ and lower by non-equilibrium fractionation during subsequent phase changes, including evaporation or freezing of moisture when ground ice formed (Lacelle et al., 2004).

The major cation concentrations (Na^+, Mg^{2+}, Ca^{2+}, K^+) of the ground-ice water samples were determined by optical emission spectrometry (inductively coupled plasma-optical emission spectrometer ICP-OES; Optima 3000 XL, PerkinElmer). The anions (Cl^-, SO_4^-) were assessed using ion chromatography (Dionex DX-320). HCO_3^- concentrations were measured immediately after rhizon sampling by titration with 0.01 M HCl using an automatic titrator (Metrohm 794 Basic Titrino). Ion concentrations are expressed in millimol-equivalents per litre (meq L^{-1}). A total of 286 samples were used for measurements and ion balance calculations using the following equation:

$$x = \left(\sum \text{cations} - \sum \text{anions}\right) / \left(\sum \text{cations} + \sum \text{anions}\right). \quad (1)$$

A relative uncertainty of less than 10 % (related to half of the sum of cations and anions) was accepted, since the overall EC in the record is low. The ionic balance uncertainty was > 10 % for only five samples, which are from between 4.0 and 8.0 m core depth.

The remaining sample parts were freeze-dried and then the absolute ice content was determined and is expressed as total water content equivalent in weight percentage (wt%) of the moist sample. The solid portion of the sample underwent a standard suite of sediment analyses, which is described elsewhere (Schwamborn et al., 2012a). Precipitation (snow and rain) and surface water from the lake and tundra ponds were sampled between early May and late August 2003.

4 Results

4.1 Sediment strata and ground-ice occurrence

The ground-ice record of core 5011-3 developed in mostly matrix-supported sandy gravel to gravelly sand (Fig. 2). The sediment interpretation of core 5011-3 concluded that the strata belong to different portions of a prograding fan delta that enters Lake El'gygytgyn from the west (Schwamborn et al., 2012a). Between 141.0 and 117.0 m core depth several thin (< 5 cm thick) sand layers intercalate with sandy gravel and are interpreted to be the bottomset facies of prodelta sediments, which were deposited in deeper water. The sandy gravel that is encountered between 117.0 and 24.3 m core depth most likely formed as a foreset facies of the debris cone in the delta front. Between 24.3 and 8.5 m core depth various thick (< 15 cm) sandy layers, especially from 24.0 to 19.0 and from 9.6 to 9.1 m core depth, are interpreted as flooding horizons from lake level highstands. The upper 9.1 m of core are interpreted to be a topset facies consisting of slope creep deposits and creek channel fill.

Overall the ground ice in 5011-3 is structure-less pore ice that mostly formed as ice cement, that is, the intrasedimental ice filled the available pore space within the sediment layers. Occasionally the ground ice formed crusts < 1 cm thick around gravel-sized clasts, or ice inclusions, where the sediment packing was looser. Some sediment samples show ice-filled cracks suggesting that ice veins healed the ruptured sediment at a postsedimentary stage when the slope was not fully frozen. These cracks are nearly vertical in orientation, commonly 1–2 cm thick and up to 10 cm long, for example, at 93.4, 70.4, 70.05, 68.4, 66.8, 64.4, 46.3, 44.5, 41.3, 40.9,

Table 1. Mean values and range (δ^{18}O, δD, d excess) for H_2O sample sets of pore ice, precipitation, and surface waters.

H_2O sample sets	δ^{18}O (‰) vs. VSMOW	δD (‰) vs. VSMOW	d excess (‰)
Pore ice HZ 7 Core 5011-3 ($n = 18$)	−19.9 (−21.9 to −17.5)	−150.7 (−170.3 to −138.0)	7.8 (1.3 to 16.6)
Pore ice HZ 6 Core 5011-3 ($n = 7$)	−17.5 (−17.8 to −17.3)	−135.2 (−137.5 to −133.5)	5.0 (4.1 to 5.9)
Pore ice HZ 5 Core 5011-3 ($n = 34$)	−18.8 (−19.7 to −17.2)	−145.1 (−153.2 to −133.5)	5.1 (2.7 to 7.6)
Pore ice HZ 4 Core 5011-3 ($n = 34$)	−19.9 (−21.1 to −19.2)	−153.4 (−161.9 to −148.0)	6.0 (5.2 to 7.0)
Pore ice HZ 3 Core 5011-3 ($n = 121$)	−22.5 (−23.0 to −21.3)	−171.2 (−175.9 to −163.4)	7.8 (5.8 to 9.6)
Pore ice HZ 2 Core 5011-3 ($n = 51$)	−22.3 (−23.0 to −21.7)	−172.2 (−176.6 to −167.3)	6.5 (5.1 to 7.5)
Pore ice HZ 1 Core 5011-3 ($n = 31$)	−21.8 (−23.0 to −17.2)	−167.5 (−170.6 to −163.1)	6.7 (4.8 to 7.5)
Pore ice (Holocene) ($n = 31$)	−19.1 (−19.9 to −18.4)	−146.6 (−151.5 to −140.4)	6.3 (3.3 to 7.7)
Pore ice cores (Late Pleistocene) ($n = 21$)	−20.2 (−20.9 to −19.6)	−154.6 (−158.7 to −147.6)	7.3 (5.6 to 9.2)
Ice wedge (late Holocene) ($n = 26$)	−22.4 (−22.8 to −19.8)	−171.0 (−181.7 to −147.8)	9.2 (7.2 to 13.3)
Ice wedge (early Holocene) ($n = 11$)	−23.5 (−25.2 to −22.7)	−179.8 (−198.1 to −171.8)	8.5 (3.6 to 10.0)
lake ice ($n = 4$)	−18.5 (−18.0 to −19.4)	−146.3 (−149.9 to −140.5)	1.8 (−0.9 to 5.5)
Rain ($n = 17$)	−14.6 (−25.9 to −6.2)	−121.9 (−202.8 to −72.9)	−4.8 (−23.1 to 5.9)
Snow ($n = 8$)	−19.8 (−28.9 to −12.7)	−152.7 (−224.4 to −97.7)	6.3 (0.2 to 11.3)
Streams*	−18.9 (−24.2 to −16.7)	−144.9 (−179.5 to 127.8)	6.7 (mean)
Lake water column*	−19.8 (mean)	−154.9 (mean)	3.4 (mean)

* Data from: Wilkie et al. (2013).

and 19.5 m core depth. Photographic examples of the sediments and ground-ice features are given in Fig. 2.

4.2 Hydrochemical zonation

Based on the hydrochemical data the core is subdivided into seven hydrochemical zones (HZs). The zones are best defined by the EC and the associated changes in ion load. The EC changes are fairly well reflected in the other measured properties and are graphically displayed in Figs. 3 and 4; in addition, δ^{18}O, δD, and d excess with mean, minimum, and maximum values are listed in Table 1. Based on EC measurements in 2000 and 2003, it was concluded that the lake is mainly fed by melt waters with low-ion content as introduced earlier; the specific conductivities in El'gygytgyn crater inlet streams were all lower than 25 µS cm^{-1} and the lake EC was around 12 µS cm^{-1} (Cremer and Wagner, 2003). Some portions of the ground ice in core 5011-3 come close to this value with EC $\sim$ 50 µS cm^{-1}, that is, ground ice of HZs 1, 2, 4, and 6 (Fig. 3). The other HZs show a higher concentration of light soluble salts with EC values of $\sim$ 100 µS cm^{-1} (i.e. in HZs 3, 5, and 7). Water forming the ground ice is mainly of the HCO_3^--(Na^++K^+)-Ca^{2+} type, with the exception of HZ 7, which is SO_4^{2-}-(Na^++K^+) type. The 5011-3 ground ice may include a lake water component and the contact of the lake water with lake sediments should have altered the hydrochemical properties. The main cations ($Na^+ + K^+$, Ca^{2+}, and Mg^{2+}) likely derive from the interaction with the host rock that builds up the El'gygytgyn crater and which is the source of the weathered debris in the area. This debris consists of volcanic rocks with rhyolite to

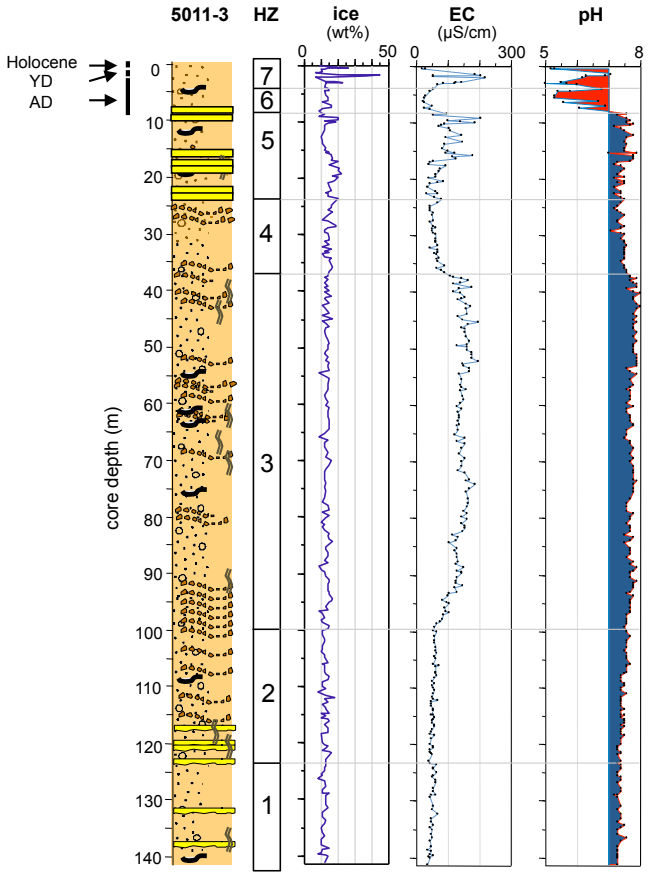

Figure 3. The lithological log of core 5011-3 with ice content, EC (electrical conductivity), and pH of the ground ice. The subdivision into hydrological zones (HZs) is based on the EC record.

andesite composition (Belyi, 1998). There is no inlet to the lake from the outside of the crater; thus, remote sources of the ion load can be excluded. HCO_3^- is estimated to originate mainly from the atmosphere via dissolution of CO_2 in lake water, since carbonate rocks are absent in the area. The modern lake water HCO_3^- is 0.90 meq L^{-1} and this is similar to the entire core ground-ice HCO_3^-, which is 0.92 meq L^{-1} [$\pm$0.48 meq L^{-1}]. Changes in sources of pore water back in time cannot be fully excluded or might be masked in the ground-ice record. However, Chapligin et al. (2012b) established a 250 ka oxygen isotope record from diatoms of the lake, which rules out to a great extent the effect of a changing hydroclimate (i.e. continentality) on the water isotope record on a multi-millennia timescale.

The small amount of Cl^- may come from the weathering of crystalline rocks (Meybeck, 1987), whereas the sulfate presumably derives from the weathering of local sulfur-bearing minerals (e.g. pyrite), since organic matter contents are low in the core (Schwamborn et al., 2012a). Ion activity coefficients are used as a measure of the interaction between the liquid and the solid phase during the process of freezing that forms ground ice. Three binary coefficients of ion activity have been calculated that are related to Ca^{2+} (K^+/Ca^{2+}, Na^+/Ca^{2+}, and Mg^{2+}/Ca^{2+}, Fig. 4). Trends in the ion activity illustrate that for much of the lower ground-ice column the relative incorporation of the Na^+ and K^+ cations into the ground ice runs parallel, although the amount of Na^+ (0.16–1.17 meq L^{-1}) is commonly 10–20 times greater than the amount of K^+ (0.01–0.09 meq L^{-1}). For Mg^{2+} (0.0–0.36 meq L^{-1}) a parallel trend is also valid for HZs 1 and 2. A slight offset occurs in HZ 3, where the fraction of Mg^{2+} is relatively higher than that of Na^+ and K^+ in the ground ice. In HZ 4 the variability of Na^+ and K^+ contents increases. In HZs 6 and 7 the variations of Na^+ and K^+ contents are greatest and only in these HZs their relative abundance is higher than that of Mg^{2+}, even though the Mg^{2+} ion has a smaller radius than Na^+ and K^+ (ion radius 10^{-12} m: $Mg^{2+} = 72$; $Ca^{2+} = 100$; $Na^+ = 102$; $K^+ = 138$). The relative amount of K^+ is highest in HZs 6 and 7. In these upper two zones K^+/Ca^{2+} shows an offset from the otherwise parallel behaviour of Na^+/Ca^{2+}. K^+ is preferentially mobilised during spring thaw (Edwards et al., 1986) and this may point to a source of this cation in the ground ice of HZs 6 and 7. Moreover, the high amounts of K^+ remarkably overlap with the zone of acidic pH in HZs 6 and 7; this acidic pH matches the modern-day snow conditions.

In the following Sects. 4.2.1–4.2.7, the zones are described from the bottom to the top.

4.2.1 HZ 1 (141.0–123.0 m)

Both water content and variability are low in this unit [12 wt% $\pm$ 1.7], the stable isotope variability is low [$\delta^{18}O$ – 21.8‰ $\pm$ 0.2; δD – 167.6‰ $\pm$ 1.4; d excess 6.7‰ $\pm$ 0.5], the slightly basic pH values show little variability [7.3 $\pm$ 1] (Fig. 3), and the EC values [51 µS cm^{-1} $\pm$ 8] and the corresponding ion load are low. Overall the water is enriched in $Na^+ + K^+$ cations over Ca^{2+} and Mg^{2+} and the anions are generally dominated by HCO_3^+ over SO_4^- and Cl^-.

4.2.2 HZ 2 (122.9–99.0 m)

Both water content and variability are low in this unit [13 wt% $\pm$ 2]. The stable isotopes are the most depleted of the entire record; that is, at 105.8 m core depth $\delta^{18}O$ min.: $-$23.0 ‰; δD min.: $-$176.7 ‰, with low stable isotope variability [$\delta^{18}O$ – 22.4‰ $\pm$ 0.4; δD – 172.4‰ $\pm$ 2.9; d excess 6.7‰ $\pm$ 0.6] including a trend towards more negative $\delta^{18}O$ and δD values towards the top of the zone. The variability of the slightly basic pH values is low [7.5$\pm$0.1]. This unit is separated from HZ 1 by a small but distinct offset towards lower EC values before they slightly increase [56 µS cm^{-1} $\pm$ 7]. The water in HZ 2 is enriched in $Na^+ + K^+$ cations and the anions are dominated by HCO_3^-.

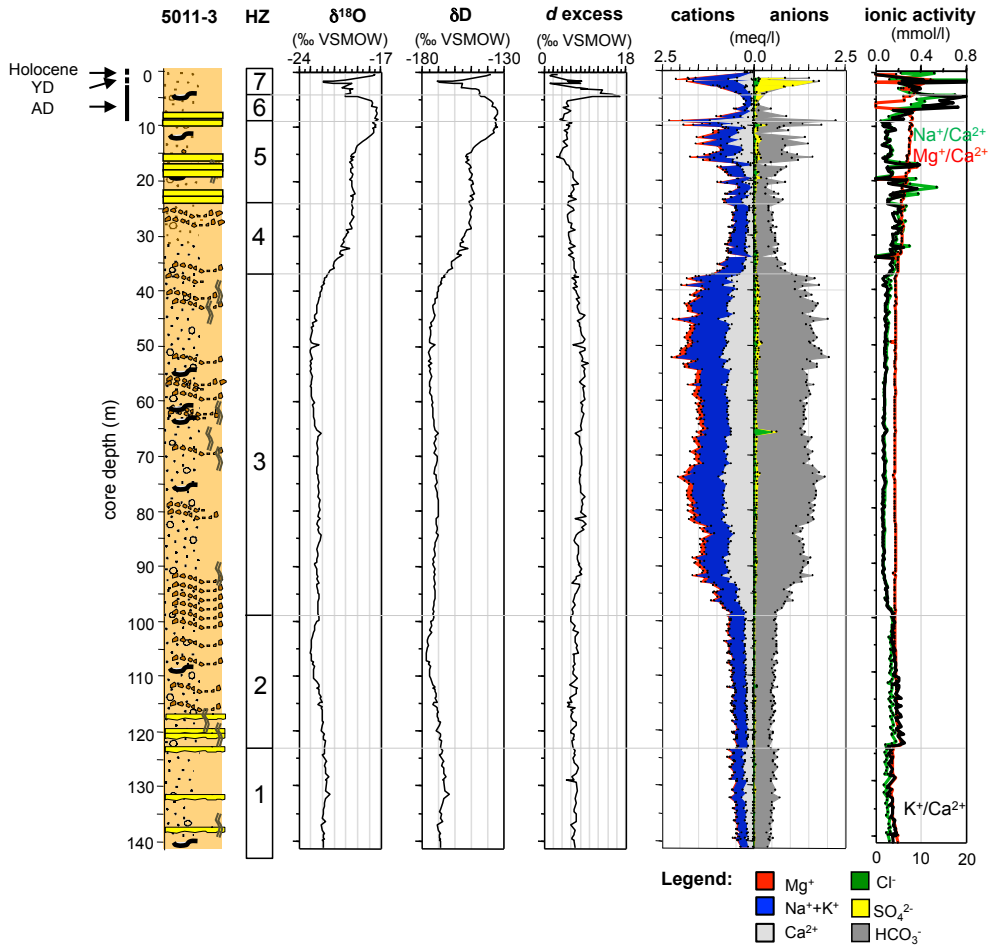

Figure 4. The lithological log of core 5011-3 with stable isotope records (δ^{18}O, δD, *d* excess), main cation and anion composition, and ion coefficients. Note: K^+/Ca^{2+} lower scale; Na^+/Ca^{2+} and Mg^+/Ca^{2+} upper scale.

4.2.3 HZ 3 (98.9–36.0 m)

Both water content and variability are low in this unit [13 wt% ± 2] and the stable isotope variations are low overall [δ^{18}O − 22.5 ‰ ± 3; δD − 172.0 ‰ ± 1.9; *d* excess 7.8 ‰ ± 0.8], although the values gently increase towards the upper part of this zone [δ^{18}O max.: −21.6 ‰; δD max.: −166.4 ‰]. With little variation pH values are slightly more basic than in the underlying zones [7.7 ± 1] and the EC values are substantially higher than in the underlying zones [140 µS cm^{-1} ± 26], hence the corresponding ion load is higher than in HZs 1 and 2 (up to 3.9 meq L^{-1} at 51.1 m core depth); $Na^+ + K^+$ are again the dominant cations and HCO_3^- is the dominant anion.

4.2.4 HZ 4 (35.9–24.0 m)

Both water content and variability are low in this unit [15 wt% ± 2]; the stable isotopic composition gradually becomes heavier from the bottom to the top of this unit [δ^{18}O − 20.1 ‰ ± 0.6, −21.4 ‰ to −19.2 ‰] [δD − 155.0 ‰ ± 4.6, −164.5 ‰ to −148.0 ‰], and the *d* excess gradually becomes smaller towards the top of this section [6.0 ‰ ± 0.6; 7.0–5.2 ‰]; and the pH values are less basic than in HZ 3 and are comparable to those in HZ 1 and 2, with little variability [7.4 ± 0.1], the EC is lower than in HZ 3 [62 µS cm^{-1} ± 13]. $Na^+ + K^+$ remain the dominant cations and HCO_3^- the dominant anion.

4.2.5 HZ 5 (23.9–8.0 m)

The water content is low in this unit with slightly greater variability than in the underlying units [15 wt% ± 4, min.: 9 wt%, max.: 22 wt%]. Including a distinct break at 13.5 m core depth the stable isotope values increase towards the top of the zone where the heaviest isotope composition of the total record occurs between 11.0 and 8.0 m core depth [δ^{18}O − 18.9 ‰ ± 0.9, −19.7 ‰ to −17.2 ‰] [δD − 145.7 ‰ ± 6.8, −153.2 ‰ to −133.5 ‰], while the *d* excess values decrease towards the top of this zone with a mean of 5.3 ‰ ± 1.1 [7.6–2.7 ‰]. The pH values are slightly higher and have higher variation than in the underlying zone [47.5 ± 0.2; 7.0–7.94].

The EC values are higher than in the underlying zone and vary to some degree [91 ± 42; 36–207]. $Na^+ + K^+$ remain the dominant cations and HCO_3^- the dominant anion.

4.2.6 HZ 6 (7.9–5.0 m)

Both water content and variability are low in this unit [13 wt% ± 2.5], the stable isotopic composition gradually becomes lighter from the bottom to the top of this unit [$\delta^{18}O - 17.5‰ \pm 0.2$; −17.8 to −17.3 ‰] [$\delta D - 135.2‰ \pm 1.7$; −137.5 to −133.5 ‰], and the *d* excess values decrease [5.0 ‰ ± 0.6; 5.9–3.4 ‰]. The pH values are acidic for the first time and show some variability [6.0 ± 0.7; 5.3–6.9]. The EC values are lower than in the underlying zone and show little variability [32 µS cm^{-1} ± 12; 23–52 µS cm^{-1}). $Na^+ + K^+$ remain the dominant cations and HCO_3^- the dominant anion.

4.2.7 HZ 7 (4.9–0.0 m)

The water content of this zone is slightly higher [16 wt% ± 10] than in the underlying zones, including individual layers with water content as high as 45 wt% (i.e. at 1.7 m core depth). The stable isotopic composition is more variable here than in any other zone; $\delta^{18}O$ [−19.8 ‰ ± 1.3] ranges between −21.9 ‰ and −17.5 ‰ and δD [−150.7 ‰ ± 10] between −170.3 ‰ and −138.0 ‰. A distinct minimum peak in δ values occurs at 1.7 m core depth, and a maximum peak occurs towards the top of this zone. The *d* excess has the highest value of the total record (+16.6 ‰) at 4.4 m depth following an abrupt transition from the lower values of the underlying HZ 6. Towards the top of HZ 7, the *d* excess values decrease to 1.3 ‰ at 2.1 m depth, before they increase again to 8.3 ‰ at 1.7 m core depth and decrease again (< 2 ‰) in the uppermost metre. The pH values are mostly acidic with little variability [5.9 ± 0.7; 5.0–7.1]. The EC values are high [98 µS cm^{-1} ± 66] with a distinct maximum peak at 2.0 m core depth (219 µS cm^{-1}) and a minimum peak at 0.4 m core depth (20 µS cm^{-1}). $Na^+ + K^+$ remain the dominant cations with the highest proportional amount of all HZs, and whereas in all other zones HCO_3^- was the dominant anion, in HZ 7 SO_4^- is dominant.

5 Discussion

5.1 Ground-ice origin: constraints from the ion composition

Mackay and Lavkulich (1974) report ion concentrations of Cl^-, Mg^{2+}, K^+, Ca^{2+}, and Na^+ in unfrozen water below the permafrost in two drained lakes near Tuktoyaktuk, western Canadian Arctic, to be 10–20 times higher than the concentrations in the surrounding ice. Experiments conducted to assess the effects of salinity on freezing front advance and solute redistribution show that solute exclusion occurs during freezing, resulting in high-solute concentration in the unfrozen pore water (Mahar et al., 1983). Kadlec (1984) reports similar observations in peat. Applied to core 5011-3, we assume that each particular freezing period that happened on the lake edge in the geologic past has left behind a ground-ice composition with a residual ionic content after the freezing front migrated through the sediments. These studies cited above are based on unidirectional freezing, mostly from the surface downward. Frost penetration in arctic soils mainly takes place from above, additional lateral and upward movement of the freezing front is expected where thawed ground (i.e. talik) below a lake is surrounded by permafrost, which is partly true for the El'gygytgyn lake edge, where permafrost surrounds the talik from three sides. The redistribution of solutes (as well as the isotopic composition) depend strongly on the freezing rate, moisture content, sediment texture, and time; thus, the proposed scheme of using ion gradients is simplistic. Because many soil surfaces are charged and the solubility of different soil minerals is highly variable and may change through time, ion mobility also depends on the specific ions (Marion, 1995). For example, Ugolini and Anderson (1973) found that Cl^- is more mobile in Antarctic soils than is Na^+ when observing the ionic movement in the unfrozen interfacial films at mineral surfaces in frozen ground. Applied to core 5011-3, a pattern of slow and then more rapid freezing might be inferred from the HZs. Freezing and ground-ice formation in HZs 1–3 presumably took place at a constant rate allowing fairly constant amounts of the main cations to be frozen in, as mirrored in the fairly uniform ion activity record of the HZs 1–3 core portion (Fig. 4). In HZs 4 and 5 the ion pattern becomes more irregular; it exhibits the highest variability in HZs 6 and 7. Here, a more rapid freezing of solute pockets in the active layer likely took place during the time when HZs 6 and 7 formed and may have led to the relative enrichment of K^+ in these HZs. Remarkably, the assumed YD stable isotope peak (as is further discussed below) at 2.5 m depth is associated with a distinct high-ion load at the same depth. Previously a similar phenomenon in the P2 record of frozen slope deposits was interpreted as an indication that high-ion concentrations in the YD ground ice preserved severe cold-climate weathering (Schwamborn et al., 2008). Possibly the breakdown of sediment particles in the course of seasonal temperature shock and cryogenic weathering (i.e. frost weathering, including ice as a weathering agent; Schwamborn et al., 2012b) increased the total surface area of grains, allowing chemical weathering to become more productive. The individual Cl^- enrichment in the sediment layer at 65.7 m depth is debatable. Possibly a lack of permeability prevented the escape of the solute inclusion from that sediment layer when the layer froze over.

5.2 Ground-ice origin: constraints from the entire core water stable isotope composition

In the $\delta^{18}O$–δD diagram (Fig. 5), the freezing process causes a deviation from the GMWL along a line with a lower slope

(a so-called freezing slope) that can be diagnostic of the conditions prevailing during freezing (Lacelle et al., 2004). During equilibrium freezing, the value of the $\delta^{18}O$–δD regression slope differs from that of the GMWL, because of different isotopic fractionation coefficients (for ^{18}O and D) during the water–ice phase change than is the case for the water-vapour fractionation. The 5011-3 ground ice has a slope of 7.5 suggesting a stable isotope history, which includes kinetic fractionation, that is, during freezing, or the impact of a changing freezing velocity or the inclusion of recycled (i.e. multiple cycles of local evaporation and condensation) water from tundra (Kurita et al., 2003) or open water surfaces in the area. Lately Lacelle (2011) concluded that ice produced by freezing of precipitation or melt water under equilibrium conditions in an open system will tend to have a slope near or greater than 7.3. In contrast, under non-equilibrium conditions an ice body found in western Canadian Arctic permafrost had a slope of 5.9 and has been interpreted to result from a complete freeze-over of a closed-system water pond in a glacier forefield after the pond had been overridden by paraglacial debris (Fritz et al., 2011).

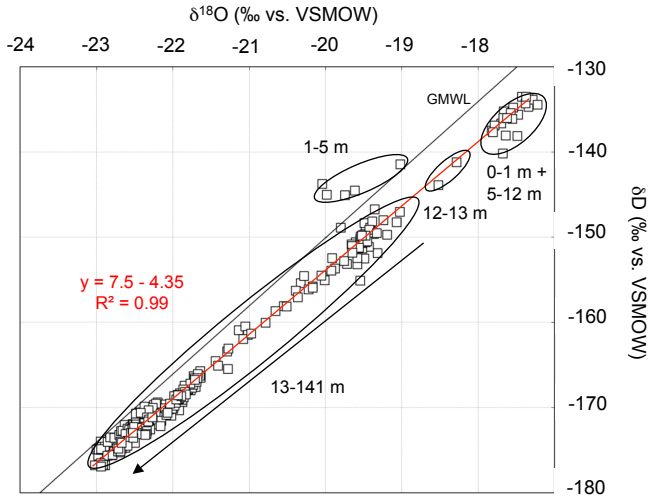

Figure 5. Stable isotope composition of core 5011-3 pore ice; GMWL (global meteoric water line) after Craig (1961).

5.3 Ground-ice origin: constraints from downcore hydrochemical and stable isotope variability and sediment data

The pH measurements of the lake water indicate that Lake El'gygytgyn is circumneutral to weakly acidic (Cremer et al., 2005). This is also true for ground ice that was retrieved with two 5 m permafrost cores in the El'gygytgyn crater (P1 and P2, see Fig. 1) and in nearby ice wedges, which all have weakly acidic pH values between 6 and 7 (Schwamborn et al., 2006). The cores P1 and P2 represent subaerial accumulations of slope deposits and date back to ~ 13 000 year BP (before present). Similar pH values (5–7) are also found in the upper core segments of 5011-3 in HZs 6 and 7. In terms of pH ,this ground-ice portion thus resembles the pH conditions of the modern lake water and near-surface permafrost elsewhere in the crater. Andreev et al. (2012) found that the sediment layers of HZ 6 and 7 are rich in pollen; a typical AD (11.2–10.7 ka BP) pollen assemblage is found in the sediment layers between 9.5 and 2.5 m core depth, a Younger Dryas (YD; 10.7–10.2 ka BP) pollen association is found between 2.5 and 1.8 m core depth, and a Holocene (10.2 ka BP to modern) pollen composition between 1.8 and 0.0 m core depth (Fig. 2). The warm-climate AD sediment layers correspond to HZ 6, including the prominent maximum peak with the most positive stable isotope composition of the core at 9.0 m core depth (Fig. 4). In contrast, the overlying cold-climate YD sediments show a distinct minimum peak in the ground-ice isotope record at 1.8 m core depth, before the second maximum peak with a heavier isotope composition appears in the warm-climate Holocene sediment layers at 0.4 m core depth. $\delta^{18}O$ and δD minima and maxima match those of the vegetation change in HZs 6 and 7 layers, and thus sediments likely contain vegetation remains and ground ice evolved from palaeo-precipitation of contemporaneous age. This holds true even with the pollen providing a summer signal, whereas the ground ice formed under subaerial conditions is fed by both winter and summer precipitation (Schwamborn et al., 2006). The hydrological history in the HZs 6 and 7 deposits therefore parallels the subaerial sediment history. When excluding a lake origin of the ground ice in HZ 7, the isotopic composition of HZ 7 is similar to the one for snow with both groups having similar mean δ values. HZ 6 is shifted towards higher mean δ values, falling between the isotopic composition of recent rain and snow. Similar overlapping histories of synsedimentary ground-ice formation where palaeo-precipitation changes are parallelled by bio-indicators during the late Quaternary are known from other terrestrial permafrost archives in northern Siberia (e.g. Schirrmeister et al., 2002, 2003; Wetterich et al., 2011; Vasil'chuk et al., 2012).

The varying d excess values in HZs 6 and 7 ranging between more than 16 and 1 ‰ (Fig. 4) indicate that during the formation time the ground ice was likely frozen and thawed various times with the palaeo-precipitation signal still being preserved. Decreasing d excess may be related to greater input from rain rather than snow into the ground-ice system, because rain may be influenced by secondary evaporation and by the recycling of regional moisture in the tundra (Kurita et al., 2003). Especially in the uppermost 5 m of core (HZ 7), secondary fractionation can also be detected with δ values above the GMWL (Fig. 5). At least one event of thermal change during the late Holocene is also seen in changes of diatom associations found in Lake El'gygytgyn sediments. They demonstrate that at about 3.6 ka BP summers warmed, resulting in longer ice-free seasons and higher bio-productivity in the lake (Cremer and Wagner, 2003). On

the land surface this coincides with the transition from the formation of a lower to an upper ice-wedge generation in slope deposits of the El'gygytgyn crater (Schwamborn et al., 2006). Hence, likely a precipitation signal changed by kinetic fractionation has been preserved in the ground ice of the slope deposits back to the AD and subaerial slope deposits have accumulated at the 5011-3 coring site since that time. For comparison, thermal change across the AD–YD–Holocene transition as expressed in increasing d excess from 5 to 10 ‰ is known from an Alaska near-surface ground-ice formation fed by palaeo-precipitation (Meyer et al., 2010a).

In contrast, the weakly basic pH found from HZs 1 to 5 (pH between 7 and 8, Fig. 3) differs from that of HZs 6 and 7 with its subaerial signature and points to a different ground-ice genesis. Depending on core depth and the HZ zonation under consideration, the stable isotope composition of ground ice has different overlaps with the compositions of other water types sampled in the area (Table 1, Fig. 6). The δ^{18}O mean values of snow and lake water (-19.8 ‰) in the El'gygytgyn crater are similar and suggest that the lake water composition is largely controlled by snow. Earlier it was stated that the lake is snowmelt fed (Cremer and Wagner, 2003) based on the low lake water EC ($< 20\,\mu S\,cm^{-1}$). In recent studies it was found that the lake water column is well mixed with low evaporation (Chapligin et al., 2012a) and the period of lake water residence time is about 100 years (Fedorov et al., 2013). An isotopic composition similar to what has been described for snow and lake water is found in particular in HZ 4 with their matching mean δ values (Fig. 6).

The stable isotope composition of HZ 5 is similar to the isotopic composition of stream input with slightly higher δ values. Wilkie et al. (2013) have specified an annual average partitioning of precipitation in El'gygytgyn crater into 60 % winter contribution and 40 % summer input (annual average $\delta^{18}O = -19.3$ ‰, $\delta D = -152.9$ ‰). Bearing in mind this estimate and also the error bars of minimum and maximum δ values in the sample sets (Table 1, Fig. 6), the possibility that rain input has influenced the formation of 5011-3 ground ice cannot be ruled out. Similarly, from the subaerial ground-ice formations found in cores P1 and P2 (Fig. 6), a two-component snow and rain input mixture has been suggested; if the mean snow and mean rain isotopic composition are considered as the two end members, the relative proportions would be 89 % snow and 11 % rain when using δ^{18}O, and 84 % snow and 16 % rain if using δD for the mixing calculations (Schwamborn et al., 2006). The isotopic composition of lake ice and streams are slightly more positive than the lake water by 1.4 and 0.9 ‰, respectively, and demonstrate that the first ice to form in autumn and the first melt water to run off in spring is enriched in ^{18}O isotopes compared to lake water.

The isotopic composition of HZs 1, 2, and 3 is similar to the one of ice wedges, especially ice wedges from the late Holocene (Fig. 6). Those ice wedges formed on subaerial slopes in the crater (Schwamborn et al., 2006) and are mainly fed by early spring snow melt water (Lachenbruch, 1962). There is no indication that ice-wedge formations have been extracted with core 5011-3 and if the ground ice in HZs 1, 2, and 3 evolved from lake water freezing instead, this would argue for colder temperatures during ground-ice development, since HZs 1, 2, and 3 exhibit the lowest δ values (δ^{18}O min.: -23 ‰; δD min.: -180 ‰) found in the 5011-3 ground-ice record. Thus, at that time the lake and the precipitation feeding it must have had considerably more negative δ values than at present, indicating environmental conditions typical of cold-climate periods. The downcore records of δ^{18}O and δD from HZs 1 to 3 exhibit fairly uniform values (δ^{18}O around -22 ‰; δ^{18}O around -170 ‰) and the combination of little isotope content variation and a stable d excess in HZs 1–3 points to a constant freezing rate of the host water in an open system (i.e. connected to the water source). In HZ 4 the δ values are 4 ‰ more positive than in HZs 1–3, and in combination with a slightly decreasing d excess from 8 to 6 ‰ suggests either different host water or a different mode of freezing when compared with the underlying zones. The same is true for the upper part of HZ 5, which is more positive by 2 ‰ in δ^{18}O. It also exhibits a continuing d excess decrease to 4 ‰. The rather linear trend of decreasing d excess can be traced between 50 and 8 m core depth, whereby the δ values show two rhythmic increases; the first one between 50 and 30 m core depth (in HZs 3 and 4), and the second one between 18 and 8 m core depth (in HZ 5). The maximum δ values occur at 8 m core depth accompanied by a d excess minimum. Consequently, freezing likely took place in at least two stages with a freezing front likely migrating from top to down and leading to an isotopically more heavy ground ice in the layers, which froze over first.

5.4 Interpretation based on permafrost and lake dynamics

At least three relative lake level highstands have reached the coring site and are marked by the $+40$, $+10$, and $+4$ m terrace, respectively (see Sect. 2). The alternation of flooding and exposure of the lake edge should have caused thawing and (re-)freezing of the ground. Times of inundation should have induced a talik formation by the thermal heat flow from the water column on top of the permafrost soil depending on water depth and timing of inundation. During the flooding events and talk formation there was potentially a lateral contact between the talik and the lake water. For comparison, a 7000 year old Lena Delta thermokarst lake is known to have developed a talik about 90 m thick below a water depth of about 10 m in a fine sandy substrate (Schwamborn et al., 2002). This study was based on seismic profiling, sediment coring, and modelling. Based on modelling results, Ling and Zhang (2003) expect a talik extension at a site in Alaska to take place within 3000 years with a maximum downward depth of 53.2 m after the formation of a shallow thaw lake with a long-term mean lake bottom temperature of

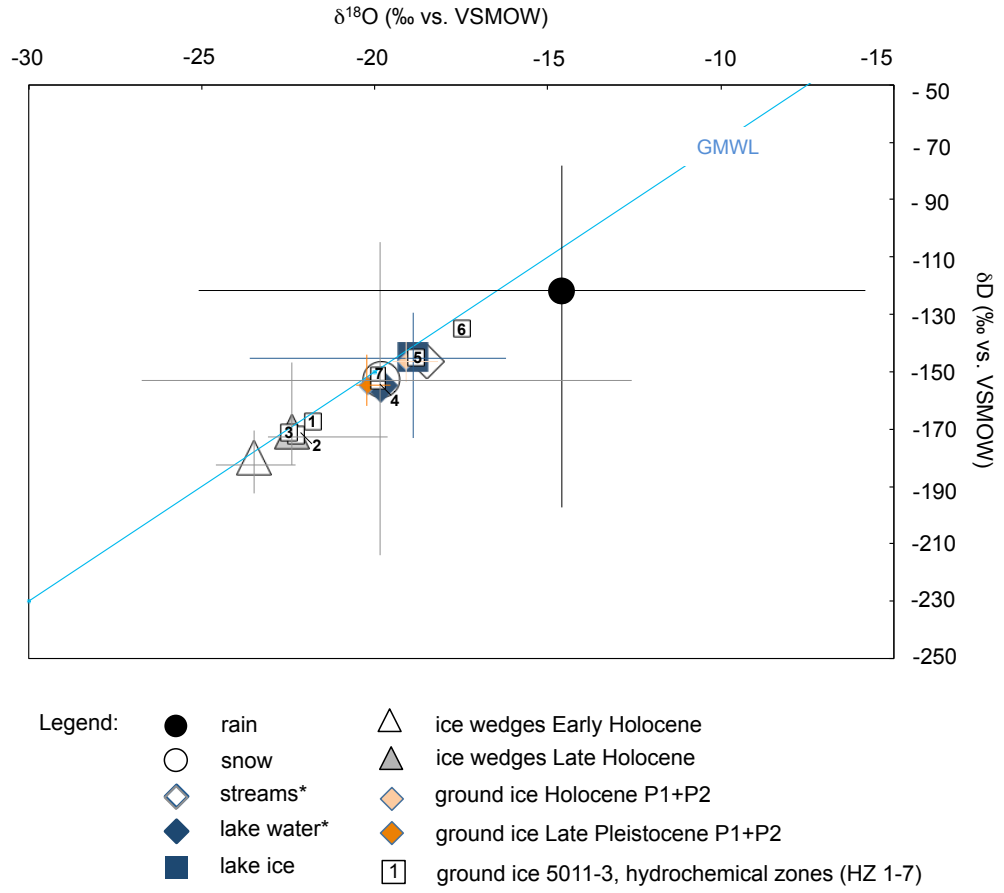

Figure 6. Stable isotope composition of 5011-3 ground ice, which is subdivided into the seven hydrochemical zones (HZs) as discussed in the text. Other H_2O sample sets from the El'gygytgyn crater are displayed for comparison with mean values and min. to max. ranges; GMWL (global meteoric water line) after Craig (1961); * data from Wilkie et al. (2013).

3.0 °C. Lake El'gygytgyn is similar to that: it has a measured temperature between 3 and 4 ° at the bottom depending on the season (Cremer and Wagner, 2003). Time and depth dimensions of those two other sites are comparable with Lake El'gygytgyn when considering past talik growth at the lake edge.

There are also at least three distinct core sections with a stable isotope record, where δ values have low variability; 105–45 m depth, 30–15 m depth, and 12–8 m depth, respectively. The ground-ice formation in these sections might be related to thaw and refreeze following the relative lake level highstands associated with the three terraces. However, repeated erosion of the sediment column at the coring site due to migrating streams in the alluvial fan system must be considered and this may have blurred at least partly the ground-ice record of thaw and refreeze. The sediment record below 9.6 m core depth is not dated and likely affected by sediment and thaw dis- and unconformities. A proper age estimate for the HZs is lacking and thus a robust history for the ground-ice formation for this core part remains speculative.

The post-LGM ground-ice history is relatively well preserved. During the LGM, the lake level was 10–12 m lower (−10 m terrace) than the modern level (Juschus et al., 2011) and thus site 5011-3 was exposed. A temperature profile of borehole 5011-3 suggests that the permafrost around the lake has inherited the temperature field from that time, since the minimum temperatures below the zone of seasonal variation are lower than can be generated by modern-day conditions. Based on forward modelling, Mottaghy et al. (2013) explained a temperature minimum of −6.7 ° at 60 m borehole depth as the result of much deeper permafrost at the end of the LGM. The amplitude of the LGM and the following warming from the Late Pleistocene to the Holocene has influenced the temperature distribution at all depths up to the surface. This means that the low-LGM temperatures have overprinted any temperature history from more ancient flooding events that warmed the ground at that time. On the other hand, ground warming during the AD and the Holocene did not erase the transient LGM temperature distribution and thus reached a depth less than 60 m.

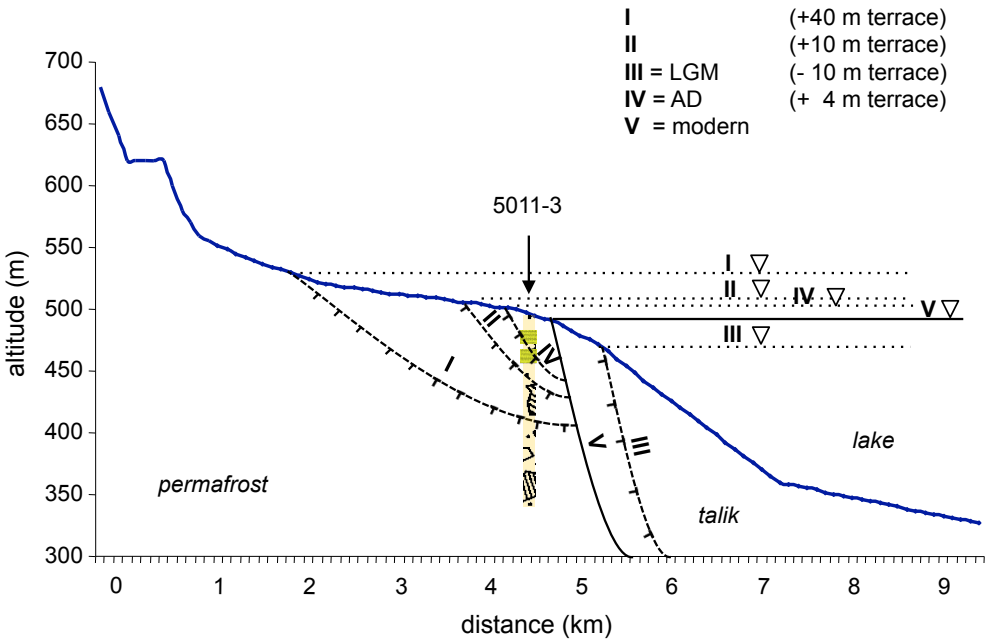

Figure 7. Interpretation of talik migration and associated repeated thaw and refreeze based on known Quaternary lake level fluctuations at the western edge of Lake El'gygytgyn. This scheme does not account for hiatuses or unconformities in the sediment and ground-ice record.

The AD age of the upper sandy beds (9.6–9.1 m core depth) in 5011-3 has been estimated from the pollen spectra (Andreev et al., 2012) and is compatible with a reconstructed lake level 3–4 m higher than modern (+4 m terrace) during that time (Schwamborn et al., 2008). After the AD flooding event the lake level dropped again and the deposits froze over. The topmost 9.1 m in the core represent slope deposits and creek fill from the AD to modern day, where migrating creeks reworked and distributed coarse-grained slope material (i.e. gravelly sand) that prograded into the lake.

Based on the obvious hydrochemical zonation of the ground ice, we propose a past freezing front migration with talik development and succeeding refreezing as illustrated in Fig. 7; it is linked to known Quaternary lake level fluctuations in the basin. However, the exact outlines of the ancient talik areas are speculative due to a lack of knowledge about sedimentation rates, dating or the presence of unconformities.

Below 9.6 m core depth the ground-ice section is likely connected to a complex history of thaw and refreeze of sediment layers as reflected in the ground-ice parameters between HZ 5 and 1. The inundation events might be linked to the exposed terraces around the lake marking ancient lake level highs and parts of the core record might have been affected by thaw and refreeze more than one time. But reconstructing a robust history of thaw and refreeze is hampered by the fact that dating of the subaerial terraces and also the relevant core portion in 5011-3 are missing. Moreover, the sedimentary record of this core portion most likely contains dis- and unconformities, because stream migration probably has affected the erosion and accumulation history in the alluvial fan system. In the same way it cannot be excluded that the postsedimentary ground-ice record has been truncated repeatedly.

6 Conclusions

Distinct changes of hydrochemical parameters of a 141 m long ground-ice record from the permafrost margin of Lake El'gygytgyn gives insight into a complex history of thaw-and-freeze at the western edge of the lake.

Zones of low variability in stable water isotope composition are interpreted to result from refreezing of former talik zones and zones of high variability in ion content point to a comparatively rapid top-down freezing process. The following downcore interpretation of the ground-ice hydrochemical changes is made:

Ground ice of precipitation origin is preserved in the upper 9.6 m of core. The ground-ice record includes palaeoclimate information from the AD, the YD, and the Holocene; it matches the principal climate history of the Eurasian Arctic during that time also mirrored by the pollen stratigraphy of the sediment layers.

The record between 141.0 and 9.6 m core depth has evolved from post-depositional thawing, including partial mixing with lake water from the neighbouring Lake El'gygytgyn in the course of lake flooding events. The isotope composition likely represents lake water, which has been overprinted by the refreezing talik.

At least three ground-ice sections in the core, which have low variability of the stable water isotope composition, might be related to past talik development and subsequent refreezing. Theoretically, they can be related to known relative lake level highstands as marked by a +40, +10, and +4 m terrace of the Middle to Late Pleistocene. A good age control for the terraces and the associated core segments is missing though.

Past thaw and freeze in the lake marginal area likely has destabilised the slope and is considered one cause of frequent sliding events, as evidenced by mass movement deposits in lake core 5011-1. Further discussion of the sedimentation processes in the deeper basin of Lake El'gygytgyn and the glacial versus interglacial turbidite record of core 5011-1 can be found in Sauerbrey et al. (2013).

Acknowledgements. Funding for this research was provided by the ICDP, the US National Science Foundation (NSF), the German Federal Ministry of Education and Research (BMBF), the Alfred Wegener Institute, Helmholtz Centre for Polar and Marine Research (AWI) and GeoForschungsZentrum Potsdam (GFZ), the Russian Academy of Sciences Far East Branch (RAS FEB), the Russian Foundation for Basic Research (RFBR), and the Austrian Federal Ministry of Science and Research (BMWF). A Russian mining rig (SIF-650M) was employed by Sergey Gutov and his crew from a local drilling company (Chaun Mining Corp., Pevek). Particular thanks go to Bernhard Chapligin and Nikifor Ostanin for help in the field. The lab support by Antje Eulenburg and Ute Bastian is highly appreciated.

Edited by: J. Brigham-Grette

References

Andreev, A. A., Morozova, E., Fedorov, G., Schirrmeister, L., Bobrov, A. A., Kienast, F., and Schwamborn, G.: Vegetation history of central Chukotka deduced from permafrost paleoenvironmental records of the El'gygytgyn Impact Crater, Clim. Past, 8, 1287–1300, doi:10.5194/cp-8-1287-2012, 2012.

Belyi, V. F.: Impactogenesis and volcanism of the Elgygytgyn depression, Petrology, 6, 86–99, 1998.

Brigham-Grette, J., Melles, M., Minyuk, P., Andreev, A., Tarasov, P., DeConto, R., Koenig, S., Nowaczyk, N., Wennrich, V., Rosén, P., Haltia, E., Cook, T., Gebhardt, C., Meyer-Jacob, C., Snyder, J., and Herzschuh, U.: Pliocene Warmth, Polar Amplification, and Stepped Pleistocene Cooling Recorded in NE Arctic Russia, Science 340, 1421–1427, doi:10.1126/science.1233137, 2013.

Chapligin, B., Meyer, H., Bryan, A., Snyder, J., and Kemnitz, H.: Assessment of purification and contamination correction methods for analysing the oxygen isotope composition from biogenic silica, Chem. Geol., 300–301, 185–199, 2012a.

Chapligin, B., Meyer, H., Swann, G. E. A., Meyer-Jacob, C., and Hubberten, H.-W.: A 250 ka oxygen isotope record from diatoms at Lake El'gygytgyn, far east Russian Arctic, Clim. Past, 8, 1621–1636, doi:10.5194/cp-8-1621-2012, 2012b.

Craig, H.: Isotopic variations in meteoric waters, Science, 133, 1702–1703, 1961.

Cremer, H. and Wagner, B.: The diatom flora in the ultra-oligotrophic Lake El'gygytgyn, Chukotka, Polar Biol., 26, 105–114, 2003.

Cremer, H., Wagner, B., Juschus, O., and Melles, M.: A microscopical study of diatom phytoplankton in deep crater Lake El'gygytgyn, Northeast Siberia, Algological Studies, 116, 147–169, doi:10.1127/1864-1318/2005/0116-0147, 2005.

Dansgaard, W.: Stable isotopes in precipitation, Tellus, 16, 436–468, 1964.

Dereviagin, A. Yu., Chizhov, A. B., Meyer, H., Hubberten, H.-W., and Siegert, Ch.: Recent ground ice and its formation on evidence of isotopic analysis, in: Proceedings of 8th International Conference on Permafrost, 21–25 July 2003, Zurich, Switzerland, 5809–5827, 2003.

Edwards, A. C., Creasey, J., and Cresser, M. S.: Soil freezing effects on upland stream solute chemistry, Water Res., 20, 831–834, 1986.

Fedorov, G., Nolan, M., Brigham-Grette, J., Bolshiyanov, D., Schwamborn, G., and Juschus, O.: Preliminary estimation of Lake El'gygytgyn water balance and sediment income, Clim. Past, 9, 1455–1465, doi:10.5194/cp-9-1455-2013, 2013.

Fritz, M., Wetterich, S., Meyer, H., Schirrmeister, L., Lantuit, H., and Pollard, W. H.: Origin and characteristics of massive ground ice on Herschel Island (western Canadian Arctic) as revealed by stable water isotope and Hydrochemical signatures, Permafrost Periglac., 22, 26–38, doi:10.1002/ppp.714, 2011.

Glushkova, O. Yu. and Smirnov, V. N.: Pliocene to Holocene geomorphic evolution and paleogeography of the Elgygytgyn Lake region, NE Russia, J. Paleolimnol., 37, 37–47, 2007.

Hallet, B.: Solute distribution in freezing ground, in: Proc. 3rd Int. Conf. Permafrost, Vol. I, National Research Council of Canada, Ottawa, Ontario, 85–91, 1978.

Juschus, O., Melles, M., Gebhardt, C., and Niessen, F.: Late Quaternary mass movement events in Lake El'gygytgyn, northeastern Siberia, Sedimentology, 56, 2155–2174, 2009.

Juschus, O., Pavlov, M., Schwamborn, G., Preusser, F., Fedorov, G., and Melles, M.: Late Quaternary lake-level changes of Lake El'gygytgyn, NE Siberia, Quaternary Res., 76, 441–451, 2011.

Kadlec, R. H.: Freezing-induced vertical solute movement in peat, in: Proc. Seventh Int. Peat Conf., 4, Irish National Peat Committee, 248–262, 1984.

Kokelj, S. V. and Burn, C.: Geochemistry of the active layer and near-surface permafrost, Mackenzie delta region, Northwest Territories, Canada, Can. J. Earth Sci., 42, 37–48, 2005.

Kurita, N., Numaguti, A., Sugimoto, A., Ichiyanagi, K., and Yoshida, N.: Relationship between the variation of isotopic ratios and the source of summer precipitation in eastern Siberia, J. Geophys. Res., 108, 4339, doi:10.1029/2001JD001359, 2003.

Lacelle, D.: On the $\delta^{18}O$, δD and D-excess relations in meteoric precipitation and during equilibrium freezing: theoretical approach and field examples, Permafrost Periglac., 22, 13–25, doi:10.1002/ppp.712, 2011.

Lacelle, D., Bjornson, J., Lauriol, B., Clark, I. D., and Troutet, Y.: Segregated-intrusive ice of subglacial meltwater origin in retrogressive thaw flow headwalls, Richardson Mountains, N.W.T., Canada, Quaternary Sci. Rev., 23, 681–696, 2004.

Lacelle, D., St-Jean, M., Lauriol, B., Clark, I. D., Lewkowicz, A., Froese, D. G., Kuehn, S. C., and Zazula, G.: Burial and preservation of a 30,000 year old perennial snowbank in Red Creek

valley, Ogilvie Mountains, central Yukon, Canada, Quaternary Sci. Rev., 28, 3401–3413, 2009.

Lachenbruch, A. H.: Mechanics of thermal contraction cracks and ice-wedge polygons in permafrost, The Geological Society of America, Special papers GSA, 70, 1–69, 1962.

Layer, P. W.: Argon-40/argon-39 age of the El'gygytgyn impact event, Chukotka, Russia, Meteorit. Planet. Sci., 35, 581–599, 2000.

Leibman, M. O.: Results of chemical testing for various types of water and ice, Yamal Peninsula, Russia, Permafrost Periglac., 7, 287–296, 1996.

Ling, F. and Zhang, T.: Numerical simulation of permafrost thermal regime and talik development under shallow thaw lakes on the Alaskan Arctic Coastal Plain, J. Geophys. Res., 108, 4511, doi:10.1029/2002JD003014, 2003.

Mackay, J. R.: Oxygen isotope variations in permafrost, Tuktoyaktuk peninsula area, Northwest Territories, Geological Survey of Canada, 83-1B, 67–74, 1983.

Mackay, J. R.: Pingo Growth and collapse, Tuktoyaktuk Peninsula Area, Western Arctic Coast, Canada: a long-term field study, Géographie physique et Quaternaire, 52, 271–323, 1998.

Mackay, J. R. and Lavkulich, L. M.: Ionic and oxygen isotopic fractionation in permafrost growth, Geological Survey of Canada, 74-1B, 255–256, 1974.

Mahar L. J., Wilson R. M., and Vinson T. S.: Physical and numerical modeling of uniaxial freezing in saline gravel, in: Proc. 4th Int. Conf. Permafrost, Nat. Acad. Press, Washington DC, USA, 773–778, 1983.

Marion, G. M.: Freeze–Thaw Processes and Soil Chemistry, U.S. Army Cold Regions Research and Engineering Laboratory 72 Lyme Road Hanover, New Hampshire 03755-1290 (CRREL), Special Report 95-12, 1–23, 1995.

Melles, M., Brigham-Grette, J., Minyuk, P. S., Nowaczyk, N. R, Wennrich, V., DeConto, R. M., Anderson, P. A., Andreev, A. A., Coletti, A., Cook, T. L., Haltia-Hovi, E., Kukkonen, M., Lozhkin, A. V., Rosén, P., Tarasov, P. E., Vogel, H., and Wagner, B.: 2.8 Million Years of Arctic climate change from Lake El'gygytgyn, NE Russia, Science, 307, 315–310, doi:10.1126/science.1222135, 2012.

Meybeck, M.: Global chemical weathering of surficial rocks estimated from river dissolved loads, Am. J. Sci., 287, 401–428, 1987.

Meyer, H., Schönicke, L., Wand, U., Hubberten, H.-W., and Friedrichsen, H.: Isotope studies of hydrogen and oxygen in ground ice: Experiences with the equilibration technique, Isot. Environ. Healt. S., 36, 133–149, 2000.

Meyer, H., Siegert, C., Derevyagin, A., Schirrmeister, L., and Hubberten, H.-W.: Paleoclimate reconstruction on Big Lyakhovsky Island, North Siberia – Hydrogen and oxygen isotopes in ice wedges, Permafrost Periglac., 13, 91–103, 2002a.

Meyer, H., Dereviagin, A. Yu., Siegert, C., and Hubberten, H.-W.: Paleoclimate studies on Bykovsky Peninsula, North Siberia – Hydrogen and oxygen isotopes in ground ice, Polarforschung, 70, 37–51, 2002b.

Meyer, H., Schirrmeister, L., Yoshikawa, K., Opel, T., Wetterich, S., Hubberten, H.-W., and Brown, J.: Permafrost evidence for severe winter cooling during the Younger Dryas in northern Alaska, Geophys. Res. Lett., 37, L03501, doi:10.1029/2009GL041013, 2010a.

Meyer, H., Schirrmeister, L., Andreev, A., Wagner, D., Hubberten, H.-W., Yoshikawa, K., Bobrov, A., Wetterich, S., Opel, T., Kandiano, E., and Brown, J.: Late Glacial and Holocene isotopic and environmental history of northern coastal Alaska results from a buried ice-wedge system at Barrow, Quaternary Sci. Rev., 29, 3720–3735, 2010b.

Michel, F. A.: Isotope characterisation of ground ice in northern Canada, Permafrost Periglac., 22, 3–12, 2011.

Mottaghy, D., Schwamborn, G., and Rath, V.: Past climate changes and permafrost depth at the Lake El'gygytgyn site: implications from data and thermal modeling, Clim. Past, 9, 119–133, doi:10.5194/cp-9-119-2013, 2013.

Niessen, F., Gebhardt, C. A., Kopsch, C., and Wagner, B.: Seismic investigation of the El'gygytgyn impact crater lake, Central Chukotka, NE Siberia, Preliminary results, J. Paleolimnol., 37, 49–63, 2007.

Nolan, M. and Brigham-Grette, J.: Basic hydrology, limnology, and meteorology of modern Lake El'gygytgyn, Siberia, J. Paleolimnol., 37, 17–35, 2007.

Opel, T., Derevyagin, A. Y., Meyer, H., Schirrmeister, L., and Wetterich, S.: Paleoclimatic information from stable water isotopes of Holocene ice wedges on the Dmitrii Laptev Strait, Northeast Siberia, Russia, Permafrost Periglac., 22, 84–100, 2011.

Ostroumov, V., Siegert, Ch., Alekseev, A., Demidov, V., and Alekseeva, T.: Permafrost as a frozen geochemical barrier, in: Proc. 7th Int. Conf. on Permafrost, Yellowknife, June 1998, edited by: Lewkowicz, A. G. and Allard, M., 855–859, 1998.

Ostroumov, V., Hoover, R., Ostroumova, N., Van Vliet-Lanoë, B., Siegert, Ch., and Sorokovikov, V.: Redistribution of soluble components during ice segregation in freezing ground, Cold Reg. Sci. Technol., 32, 175–182, 2001.

O'Sullivan, J. B.: Geochemistry of Permafrost: Barrow, Alaska, in: Proc. Intern. Conf. Permafrost, Lafayette, Indiana, Natl. Acad. Science, Washington DC, 30–37, 1963.

Qiu, G., Sheng, W., Huang, C., and Zheng, K.: Direction of ion migration during cooling and freezing processes, in: Proc. Fifth Int. Conf. Permafrost, Trondheim, Norway, August 1988, 442–447, 1988.

Rozanski, K., Araguás-Araguás, L., and Gonfiantini, R.: Isotopic patterns in modern global precipitation, in: Climate Change in Continental Isotopic Records, edited by: Swart, P. K., Lohmann, K. C., Mckenzie, J., and Savin, S., AGU, Washington, D.C., Geophys. Monogr. Ser., 78, 1–36, doi:10.1029/GM078p0001, 1993.

Sauerbrey, M. A., Juschus, O., Gebhardt, A. C., Wennrich, V., Nowaczyk, N. R., and Melles, M.: Mass movement deposits in the 3.6 Ma sediment record of Lake El'gygytgyn, Far East Russian Arctic, Clim. Past, 9, 1949–1967, doi:10.5194/cp-9-1949-2013, 2013.

Schirrmeister, L., Siegert, C., Kuznetsova, T., Kuzmina, S., Andreev, A. A., Kienast, F., Meyer, H., and Bobrov, A.: Paleoenvironmental and paleoclimatic records from permafrost deposits in the Arctic region of Northern Siberia, Quatern. Int., 89, 97–118, 2002.

Schirrmeister, L., Grosse, G., Schwamborn, G., Andreev, A. A., Meyer, H., Kunitsky, V. V., Kuznetsova, T. V., Dorozhkina, M. V., Pavlova, E. Y., Bobrov, A. A., and Oezen, D.: Late Quaternary history of the accumulation plain north of the Chekanovsky Ridge (Lena Delta, Russia): a multidisciplinary approach, Polar Geography, 27, 277–319, 2003.

Schwamborn, G., Andreev, A., Rachold, V., Hubberten, H.-W., Grigoriev, M. N., Tumskoy, V., Pavlova, E. Y., and Dorozhkina, M. V.: Evolution of Lake Nikolay, Arga Island, Western Lena River delta, during Late Pleistocene and Holocene time, Polarforschung, 70, 69–82, 2002.

Schwamborn, G., Meyer, H., Fedorov, G., Schirrmeister, L., and Hubberten, H.-W.: Ground ice and slope sediments archiving Late Quaternary paleoenvironment and paleoclimate signals at the margins of El'gygytgyn Crater, NE Siberia, Quaternary Res., 66, 259–272, 2006.

Schwamborn, G., Fedorov, G., Schirrmeister, L., Meyer, H., and Hubberten, H.-W.: Periglacial sediment variations controlled by Late Quaternary climate and lake level rise at El'gygytgyn Crater, Arctic Siberia, Boreas, 37, 55–65, 2008.

Schwamborn, G., Fedorov, G., Ostanin, N., Schirrmeister, L., Andreev, A., and the El'gygytgyn Scientific Party: Depositional dynamics in the El'gygytgyn Crater margin: implications for the 3.6 Ma old sediment archive, Clim. Past, 8, 1897–1911, doi:10.5194/cp-8-1897-2012, 2012a.

Schwamborn, G., Schirrmeister, L., Frütsch, F., and Diekmann, B.: Quartz weathering in freeze–thaw cycles: experiment and application to the El'gygytgyn Crater Lake record for tracing Siberian permafrost history, Geogr. Ann. A, 94, 481–499, doi:10.1111/j.1468-0459.2012.00472.x, 2012b.

Seeberg-Elverfeldt, J., Schlüter, M., Feseker, T., and Kölling, M.: Rhizon sampling of pore waters near the sediment/water interface of aquatic systems, Limnol. Oceanogr.-Meth., 3, 361–371, 2005.

Souchez, R. A., Jouzel, J., Lorrain, R., Sleewaegen, S., Stiévenard, M., and Verbeke, V.: A kinetic isotope effect during ice formation by water freezing, Geophys. Res. Lett., 27, 1923–1926, 2000.

Stuiver, M. and Yang, I. C.: Oxygen isotope ratios of Antarctic permafrost and glacier ice, in: Antarctic Research Series 33, Dry Valley Drilling Project, American Geophysical Union, DC, 131–139, 1981.

Swanger, K. M., Marchant, D. R., Kowalewski, D. E., and Head, J. W.: Viscous flow lobes in central Taylor Valley, Antarctica: Origin as remnant buried glacial ice, Geomorphology, 120, 174–185, 2010.

Ugolini, E. C. and Anderson, D. M.: Ionic migration and weathering in frozen Antarctic soils, Soil Sci., 115, 461–470, 1973.

Vasil'chuk, Yu. K., Vasil'chuk, A. C., and Budantseva, N. A.: Isotopic and palynological compositions of a massive ice in the Mordyyakha River, Central Yamal Peninsula, Dokl. Earth Sci., 446, 1105–1109, 2012.

Wetterich, S., Rudaya, N., Tumskoy, V., Andreev, A. A., Opel, T., Schirrmeister, L., and Meyer, H.: Last Glacial Maximum records in permafrost of the East Siberian Arctic, Quaternary Sci. Rev., 30, 3139–3151, 2011.

Wilkie, K. M. K., Chapligin, B., Meyer, H., Burns, S., Petsch, S., and Brigham-Grette, J.: Modern isotope hydrology and controls on δD of plant leaf waxes at Lake El'gygytgyn, NE Russia, Clim. Past, 9, 335–352, doi:10.5194/cp-9-335-2013, 2013.